

Superfluid Fraction of ^3He - ^4He Mixtures Confined at $0.0483 \mu\text{m}$ Between Silicon Wafers

Mark O. Kimball and Francis M. Gasparini
University at Buffalo, SUNY Buffalo, NY 14260, USA

We report measurements of the superfluid fraction ρ_s/ρ of films of ^3He - ^4He mixtures confined between silicon wafers at $0.0483 \mu\text{m}$ separation. The data obtained using Adiabatic Fountain Resonance (AFR) can be used to test for the first time expectations of correlation-length scaling in the case of *planar* mixtures. For the mixtures, the data for ρ_s/ρ collapse well on a universal function. The dissipation associated with AFR can also be scaled, and indicates two-dimensional crossover. These results are in contrast to pure ^4He , where over a wider range of confinements, the data for ρ_s/ρ are found not to scale.

The behavior of a system near a second order phase transition when confined to a small spatial dimension is a fundamental problem in statistical mechanics [1–4]. If the spatial confinement is uniform at some small length scale L , one expects that the critical behavior will be renormalized in a way which should be described by scaling functions. These involve only the critical properties of the system of interest as obtained in the thermodynamic limit. Further, specific to a given confinement geometry, one may obtain behavior which reflects dimensionality crossover. For instance, a film geometry would show two-dimensional (2D) crossover. Scaling functions describing this would depend only on the ratio of L to the correlation length ξ of the unconfined system except in the 2D region.

There has been a substantial amount of work on ^4He at the superfluid transition to address these issues [5]. For the specific heat in particular, recent work has shown good agreement with scaling predictions and qualitative agreement with calculated scaling functions [6–10]. There are difficulties which still remain on the superfluid side, especially near the specific heat maximum [7,8]. In the case of the superfluid fraction for planar confinement the situation is not as good. Measurements for ^4He for 2D crossover have shown lack of scaling which remains unexplained [11]. On the theory side, Monte Carlo simulations of the XY model have also shown lack of scaling which could be fixed by introducing an additional length scale to the scaling equations [12]. Field theory calculations yield a unique scaling function [13].

Much less is known experimentally for the finite-size scaling of ^3He and ^4He mixtures. These present an opportunity to study finite-size scaling by using the *same spatial confinement* and varying the ^3He molar concentration x . This makes use of the fact that the magnitude of the correlation length ξ for mixtures varies with concentration while the critical exponent is universal, at least for small x . Specifically, one has [14–16]

$$\xi = \frac{m_4^2 k_B T}{4\pi \hbar^2 \rho} \left(\frac{\rho}{\rho_s} \right) = \xi_0 t^{-\nu} \quad (1)$$

where $t = (1 - T/T_\lambda)$, $\nu = 0.671$ [17], and ρ_s/ρ behaves as

$$\frac{\rho_s}{\rho} = k(x) t^\nu \quad (2)$$

Thus, the amplitude of the correlation length at any ^3He concentration is given by

$$\frac{\xi_o(x)}{\xi_o(0)} = \frac{T_\lambda(x)\rho(0)k(0)}{T_\lambda(0)\rho(x)k(x)} \quad (3)$$

Eq. 3 allows one to explore ranges of $\xi_o(x)$ over a factor of about 2 before one runs into thermodynamic path effects associated with measurements at constant concentration rather than constant chemical potential difference [18–20]. Measurements of the superfluid fraction for cylindrical confinement have been done, however, these data have not yielded an overall scaling [21].

To achieve confinement, we have used a technique whereby two wafers of silicon are bonded at a separation determined by a lithographically-formed pattern of SiO_2 [22,23]. This yields a uniform enclosure for the confined helium. For the cell used in this work $L = 0.0483 \mu\text{m}$, and the lateral extent is about 2 cm. Thus, helium confined in this cell is a film bounded by two solid surfaces and, effectively, infinite lateral extent. We have reported heat capacity measurements using several of these cells with various values of L up to $0.9869 \mu\text{m}$ [6–8].

To measure the superfluid density we make use in the present work of a resonance in the motion of the superfluid. This involves movement of the superfluid between the cell, which acts as a superleak, and a small volume in the filling line with which the helium communicates [24]. This motion is driven thermally by applying an AC signal to a heater. We have called this Adiabatic Fountain Resonance. It is a Helmholtz resonance in which the restoring force for the movement of the helium is provided

by differences in the chemical potential between the helium in the cell and the filling line. Thus, there is an oscillatory response in the temperature, pressure, and in the case of mixtures, concentration. In our experiment, we detect the temperature oscillations.

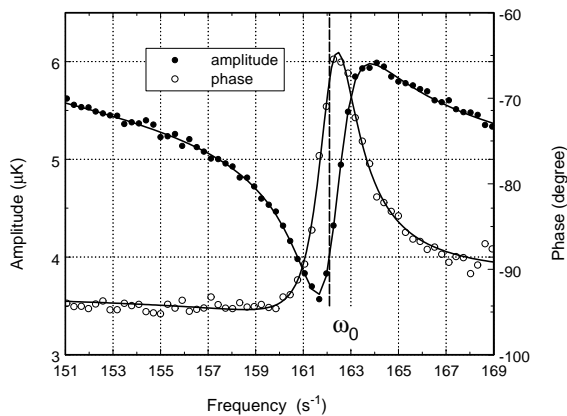


FIG. 1. Example of AFR resonance, temperature and phase shift as function of drive frequency. The solid lines are fits to Eqs. 5, 6

The derivation of the resonance frequency for pure ^4He was reported in [24]. For the case of mixtures, a similar procedure [25] can be followed to obtain for the resonance frequency ω_R

$$\omega_R^2 = \frac{\rho_s}{\rho} \frac{\sigma}{l_P \rho V K} (1 + \alpha - \beta) = \omega_0^2 (1 + \alpha - \beta) \quad (4)$$

where σ and V are geometric parameters of the cell, K is the isothermal compressibility, and l_P is a length over which the pressure varies between the filling line and the confined helium in the cell. The thermodynamic parameters α and β are most easily derived as function of the mass concentration. They involve a number of thermodynamic derivatives which can be evaluated. We find that $(\alpha - \beta)$ varies between $+0.02$ and -0.07 for the range of concentrations we have studied. In particular, $\alpha(T, x)$ reduces to the expression of α at $x=0$ given in [24]; and, $\beta(T, x)$ vanishes at $x=0$. The frequency ω_0 , which contains the superfluid fraction, can be obtained from our measurements by analyzing the response of the cell as a function of drive frequency ω . One finds [25] that the amplitude of the temperature oscillations is given by

$$\tau_0 = a_0 \frac{\cos(\tan^{-1} \frac{(1+\alpha-\beta)\omega\omega_0^2 - \omega^3 + \mathcal{L}\Lambda\omega}{\mathcal{L}(\omega_0^2 - \omega^2) - \Lambda\omega^2})}{-\omega \sin(\tan^{-1} \frac{\Lambda\omega}{\omega_0^2 - \omega^2}) + \mathcal{L} \cos(\tan^{-1} \frac{\Lambda\omega}{\omega_0^2 - \omega^2})} \quad (5)$$

while the phase difference θ , between the drive signal and the detected signal, is given by

$$\tan\theta = \frac{\omega(\omega_0^2 - \omega^2)[(1 + \alpha - \beta)\omega_0^2 - \omega^2] + \Lambda^2\omega^3}{\mathcal{L}(\omega_0^2 - \omega^2)^2 + (\alpha - \beta)\Lambda\omega_0^2\omega^2 + \mathcal{L}\Lambda^2\omega^2} \quad (6)$$

In these two equations \mathcal{L} and Λ are scaled quantities with dimensions s^{-1} which are related to the thermal conductivity and dissipation respectively [24].

In Fig. 1 data are shown for the amplitude of the temperature response and phase shift for a concentration of $x=0.36$, at $t=(1-T/T_\lambda(x))=0.01$. The solid lines are fits of these data using Eqs. 5, 6. These fits can be done with no systematic residuals. All parameters can be obtained independently from either the phase or the temperature oscillations. In particular, ω_0 from which the superfluid fraction can be obtained is indicated in this plot with a dashed line. Note that ω_0 is not at any obvious point in these curves but is close to the maximum in the phase. The total temperature excursion measured for these data is only $2.5 \mu\text{K}$. This can be resolved to better than 50 nK . We achieve this by regulating the *average temperature* of the cell and signal-averaging at each frequency the AC oscillations associated with the resonance.

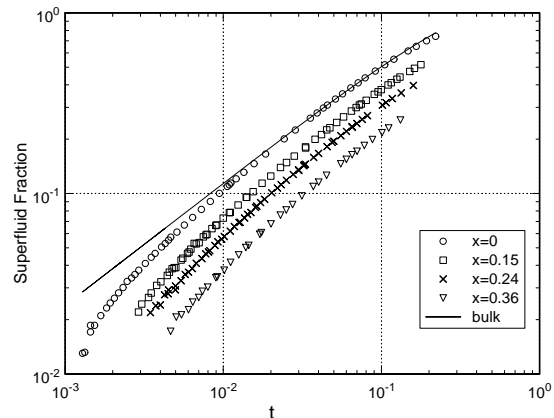


FIG. 2. Superfluid fraction for helium confined in $0.0483 \mu\text{m}$, and several concentrations.

To obtain the superfluid fraction from measurements at various concentrations, we normalize ω_0 . This is done far from the transition where the data match the behavior of unconfined helium. We have used the data from [21]. We show the result of this in Fig. 2. Here are plotted data at $x=0$ and three other concentrations. The solid line represents the data from [26]. The overall behavior of these data is qualitatively as expected: as x increases, the effect of confinement is felt at larger values of t . In particular note that at higher concentrations one cannot obtain data for smaller values of t because of the broadening of the resonance due to dissipation [27]. Ideally one should see a discontinuity in the superfluid fraction indicative of the Kosterlitz-Thouless nature of the two-dimensional crossover [28]. The $x=0$ data stop at a value only 10% higher than this expected universal discontinuity.

ity The dissipation parameter Λ ranges from $0.01 \times \omega_0$ at low temperatures, to $0.4 \times \omega_0$ when the resonance is lost.

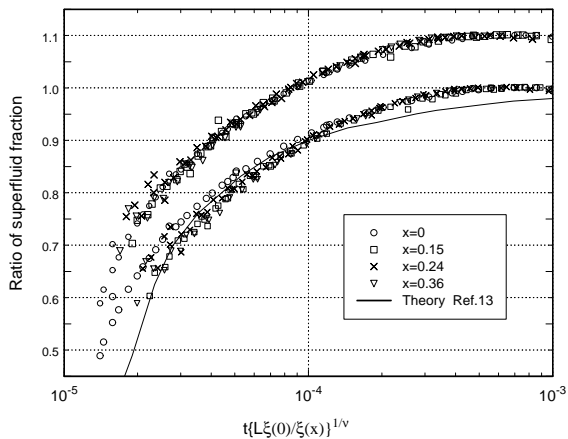


FIG. 3. Ratio of confined to bulk superfluid fractions plotted according to Eq. 7 with $\nu=0.671$ [17]. Two values of L are used in this plot. See text. The top plot is shifted upward by 0.1 for clarity.

The expected finite-size scaling of the data shown in Fig. 2 can be written in terms of a scaling function G as follows,

$$\begin{aligned} \left(\frac{\rho_s}{\rho}\right)_L &= \left(\frac{\rho_s}{\rho}\right)_{bulk} G(tL(x)^{1/\nu}) \\ &= \left(\frac{\rho_s}{\rho}\right)_{bulk} g(t(L\xi_0(0)/\xi_0(x))^{1/\nu}) \end{aligned} \quad (7)$$

where the last expression is written in such a way as to indicate that the effective confinement for the mixtures is smaller, i.e. $\xi_0(x) > \xi_0(0)$. For the concentrations we have studied, $x=0, 0.15, 0.24, 0.36$ we have $\xi_0(x)=3.57, 4.53, 5.31, 6.72$ [21]. The data plotted according to Eq. 7 are shown in Fig. 3. Two plots are generated. For the bottom plot, L is taken for all the data as the geometrical separation of the silicon wafers. The collapse of these data is quite good, however, there seems to be still some separation for the mixtures relative to the pure system. This is especially visible for small values of the scaling variable. For the top plot in this figure, which is shifted upward by 0.1, we have taken for the mixtures an effective geometrical separation of $L_{eff} = 0.9L$. A decrease in L for the mixtures relative to pure ${}^4\text{He}$ may be understood as follows. Near a confining wall there exists both a pressure gradient and a concentration gradient. This latter is due to the van der Waals field plus the greater kinetic energy of ${}^3\text{He}$ atoms relative to ${}^4\text{He}$. This gradient in x is partly in a region where the superfluid is normal, even though rich in ${}^4\text{He}$. This mechanism effectively limits the mixture to an L_{eff} smaller than L . This effect can be estimated using a continuous model [29]. Irrespective of these refinements, it is clear that the

finite-size scaling prediction based on the same geometrical confinement, but a changing $\xi_0(x)$, works well. An attempt of scaling the data without taking this into account does not work at all. Also shown in Fig. 3 is the locus of the theoretical scaling function [13]. Although this seems to have a somewhat different dependence on the scaling variable than the data, the overall magnitude seems correct.

One can also look at the dissipation associated with the resonance. The ratio of the dissipation parameter Λ to the resonance frequency ω_0 is plotted in Fig. 4 as a function of the scaling variable. One can see that the dissipation scales as well as the superfluid density in the region close to the transition. To achieve this, we have had to add to the mixture, relative to $x=0$, a constant background dissipation of $\Lambda/\omega_0=0.01$. The rapid rise in dissipation as ρ_s vanishes is indicative of vortex pair unbinding for 2D crossover. One can fit these data reasonably with the expected dissipation [27] near the 2D transition. This is the solid line in Fig. 4. This is interesting because *the data collapse using the 3D correlation length, while the locus is determined by the 2D correlation length.*

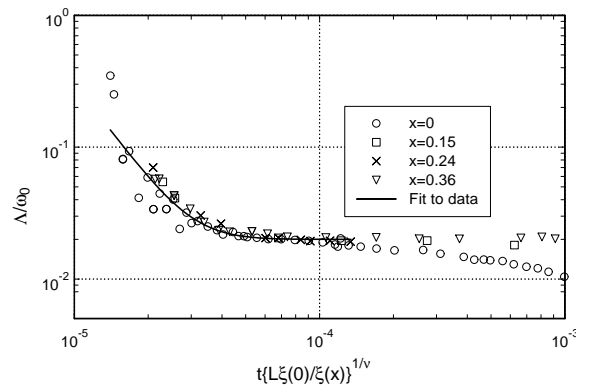


FIG. 4. Ratio of dissipation to resonance frequency as a function of the scaling variable.

We emphasize that while the scaling for the superfluid fraction and dissipation seems to work, the range of geometrical sizes tested via the variation in $\xi_0(x)$ is limited. A comparison of ρ_s/ρ over a wider range of L 's is shown in Fig. 5. These are all data for *pure* ${}^4\text{He}$. The present data and those from [24] are obtained using the AFR technique. The other data are obtained using a torsional oscillator (TO) [11]. It seems clear that collectively, over a factor of 80 in L , these data do not collapse on a universal function as expected. The AFR data seem to have a slightly different overall dependence than the TO data. But overall, there is a trend for the data at smaller confinement to lie at smaller values of the scaling variable. We also note that the AFR data at

0.0483 μm are the most affected by the Van der Waals field at the walls. *This field breaks correlation-length scaling.* However, were one to correct for this effect, *the data at smaller confinements would separate further from the data at larger confinements,* and make the disagreement with scaling even worse [30,31]. This disagreement with correlation-length scaling on the *superfluid side* of the transition has also been observed for the specific heat in the case of *planar films* [7,8].

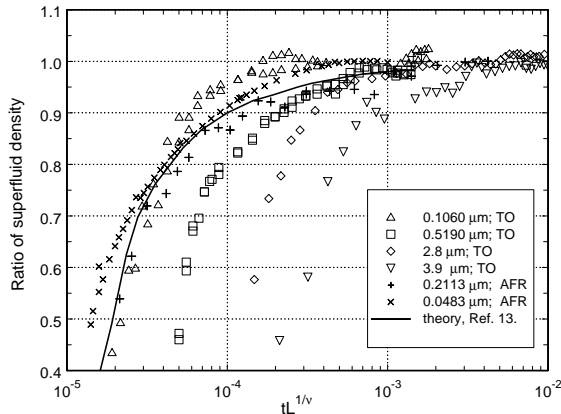


FIG. 5. Ratio of superfluid density at $x=0$ for planar confinement

In summary, we have presented data for the superfluid fraction of $^3\text{He} - ^4\text{He}$ mixtures confined in a film geometry of 0.0483 μm . The data can be used to check on correlation-length scaling by making use of the dependence of the correlation length on ^3He concentration. We find that this works both for the superfluid density and the dissipation. However, we point out that if one examines data over larger variations in confinement, as available at $x=0$, one still finds lack of scaling.

ACKNOWLEDGMENTS

This work is supported by the NSF, DMR99722287.

[1] M. E. Fisher, *Critical Phenomenon, Proc. 51st "Enrico Fermi" Summer School, Varenna, Italy*, Academic Press, NY, 1971.
 [2] M. E. Fisher and M. N. Barber, *Phys. Rev. Lett.* **28**, 1516 (1972).
 [3] M. N. Barber, *Phase Transitions and Critical Phenomena*, volume vol.8, Academic Press, New York, 1983.

[4] V. Privman, *Finite Size Scaling and Numerical Simulations of Statistical Systems*, World Scientific, NJ, 1990.
 [5] F. M. Gasparini and I. Rhee, *Progress in Low Temperature Physics*, North Holland, NY, 1992.
 [6] S. Mehta and F. M. Gasparini, *Phys. Rev. Lett.* **78**, 2596 (1997).
 [7] S. Mehta, M. O. Kimball, and F. M. Gasparini, *J. Low Temp. Phys.* **114 Nos. 5/6**, 467 (1999).
 [8] M. O. Kimball, S. Mehta, and F. M. Gasparini, *J. Low Temp. Phys.* **121 Nos. 1/2**, 29 (2000).
 [9] J. A. Lipa et al., *J. Low Temp. Phys.* **113 Nos. 5/6**, 849 (1998).
 [10] J. A. Lipa et al., *Phys. Rev. Lett.* **84**, 4894 (2000).
 [11] I. Rhee, F. M. Gasparini, and D. J. Bishop, *Phys. Rev. Lett.* **63**, 410 (1989).
 [12] N. Schultka and E. Manousakis, *Czechoslovak J. of Phys.* **46**, 451 (1996).
 [13] R. Schmolke, A. Wacker, V. Dohm, and D. Frank, *Physica B* **575**, 165 (1990), See also, V. Dohm, *Physica Scripta* vol. **T49**, 46-58 (1993).
 [14] R. A. Ferrell, N. Menyhard, H. Schmidt, F. Schwabl, and P. Szépfalussy, *Ann. Phys. (N.Y.)* **47**, 565 (1968).
 [15] B. I. Halperin and P. C. Hohenberg, *Phys. Rev.* **177**, 952 (1969).
 [16] M. E. Fisher, M. N. Barber, and D. Jasnow, *Phys. Rev. A* **8**, 1111 (1973).
 [17] L. S. Goldner and G. Ahlers, *Phys. Rev. B* **45**, 131 (1992), See also: L. S. Goldner, N. Mulders and G. Ahlers *J. Low Temp. Phys.* **93**, Nos. 1/2, 131 (1993); D. S. Greywall and G. Ahlers *Phys. Rev. A* **7**, 2145 (1973); G. Ahlers *Physica B* **107**, 347 1981; D. Marek, J. A. Lipa and D. Phillips *Phys. Rev. B* **38**, 4465 (1988); D. R. Swanson, T. C. P. Chui and J. A. Lipa *Phys. Rev. B* **46**, 9043 (1992); M. Campostrini, A. Pelissetto, P. Rossi and E. Vicari *Phys. Rev. B* **01** 5905 (2000).
 [18] G. Terui and A. Ikushima, *Phys. Lett. A* **31**, 161 (1972).
 [19] A. Ikushima and G. Terui, *J. Low Temp. Phys.* **10**, 397 (1973).
 [20] G. Ahlers, *Phys. Rev. A* **10**, 1670 (1974).
 [21] P. C. Schubert and W. Zimmermann Jr., *J. Low Temp. Phys.* **41 Nos. 1/2**, 177 (1981).
 [22] S. Mehta et al., *Czech. J. Phys.* **46**, 133 (1996).
 [23] I. Rhee, D. J. Bishop, A. Petrou, and F. M. Gasparini, *Rev. Sci. Instrum.* **61**, 1528 (1990).
 [24] F. M. Gasparini and S. Mehta, *J. Low Temp. Phys.* **110 Nos. 1/2**, 293 (1998).
 [25] F. M. Gasparini, to be published.
 [26] D. S. Greywall and G. Ahlers, *Phys. Rev. A* **7**, 2145 (1973).
 [27] V. Ambegakar, B. I. Halperin, D. R. Nelson, and E. D. Siggia, *Phys. Rev. B* **21**, 1806 (1980).
 [28] D. R. Nelson and J. M. Kosterlitz, *Phys. Rev. Lett.* **39**, 1201 (1977).
 [29] M. Chester, J.-P. Laheurte, and J.-P. Romagnan, *Phys. Rev. B* **14**, 2812 (1976).
 [30] X. F. Wang, I. Rhee, and F. M. Gasparini, *Physica B* **165-166**, 503 (1990).
 [31] K. P. Mooney and F. M. Gasparini, to be published.